63-2-3



# AIR FORCE INSTITUTE OF TECHNOLOGY

AIR UNIVERSITY
UNITED STATES AIR FORCE

## SCHOOL OF ENGINEERING

WRIGHT-PATTERSON AIR FORCE BASE, OHIO



AF-WP-O-MAY 62 5,000

THESIS

Presented to the Faculty of the School of Engineering of
the Air Force Institute of Technology
Air University
in Partial Fulfillment of the
Requirements for the Degree of
Master of Science

# AN ANALYSIS OF THE UNIPOLAR TRANSISTOR AS A CHOPPER AMPLIFIER

(Unclassified)

By
James Ray Wolverton, B. S.
Captain USAF
GE/EE/62-21

Graduate Electrical Engineering
December 1962

## Preface

This work was suggested by Mr. Neil DiGiacamo and Lieutenant Frederick Kamp of the Electronics Technology Laboratory of Wright-Patterson Air Force Base. The need for a solid state impedance transforming device became obvious as the work on a sensitive photovoltaic visible sensor approached fruition. At the same time, solid state manufacturing techniques improved to the point where unipolar field effect transistors could be made. Initially this work was to be a theoretical analysis to determine if the unipolar transistor could be used as a chopper amplifier, but since experimental devices were available at the Electronics Technology Laboratory, the work was expanded to include laboratory testing of theoretically possible circuitry. As a very definite Air Force requirement exists for a solid state celestial tracking system and sufficient devices were available to test the theory, the entire work was oriented so as to produce an operating celestial body tracking system.

I am indebted to Captain R. A. Hannen, Professor Jerzy Lubelfeld, and Captain Matthew Kabrisky of the Air Force Institute of Technology: to Captain Hannen for his long suffering patience and sound advice as thesis advisor, to Professor Lubelfeld for his cantankerous, but friendly, guidance as an engineering scientist, and to Captain Kabrisky for his accurate troubleshooting.

I am deeply indebted to Mr. Donald C. Robertson of the Dayton Art Institute who assisted in the preparation of the numerous charts and drawings contained herein. Without his artistic skill the presentation of complicated vector relationships would have been almost impossible. I wish to thank Lieutenant Kamp and Mr. DiGiacamo for their advice and their ability to uncover important facts concealed in research proposals or interim technical reports which were not available through a normal literature search. I also thank my wife and two year old son for their unflagging patience and moral support during this difficult eighteen month program.

## Contents

## Contents

## List of Figures

## List of Symbols

| Symbol | |
|---|---|
| cm | Centimeter |
| $cm^2$ | Square Centimeters |
| CRO | Cathode Ray Oscilloscope |
| $g_m$ | Change in Channel Current $I_c$ with Respect to Change in Gate Voltage $V_g$ |
| $I_d$ | Channel Current of the Unipolar Transistor |
| $I_o$ | Reverse Saturation Current of a Photodiode |
| $^oK$ | Temperature in Degrees Kelvin |
| LOP | Line of Position |
| mw | Milliwatts |
| $\theta$ | Angle Measured from X Axis to LOP in the XY Plane |
| $\phi$ | Angle Measured from Z Axis to LOP in XZ Plane |
| r | Angle Measured from Y Axis to LOP in YZ Plane |
| $R_d$ | Channel Resistance of a Unipolar Transistor |
| RMS | Root Mean Square |
| $V_g$ | Voltage at Gate of a Unipolar Transistor Measured with Respect to the Source |
| $W_o$ | Pinch-off Voltage of a Unipolar Transistor |

## Abstract

Absolute sensitivity requirements and system functions are developed for a system capable of tracking a second magnitude star. Space-compatability is defined. The problems of star acquisition and position readout are analyzed. Available photovoltaic devices, unipolar field effect transistors, servo motors, and servo power amplifiers are discussed. A method of electronic chopping using the unipolar transistor is devised. A complete star tracking system is synthesized and the method of testing and test conditions described. Results of the generally satisfactory testing are given together with recommendations for future development.

GE/EE/62-21

# AN ANALYSIS OF THE UNIPOLAR TRANSISTOR AS A CHOPPER AMPLIFIER

## I. Introduction

Certain Air Force and NASA missions have generated a requirement for a "space-compatible" celestial tracking system. The term space-compatible implies system components with low power consumption, low weight, small size, radiation resistance, and relative temperature insensitivity, and generally indicates that a solid state system should be developed. The paucity of zero and first magnitude stars, and their placement on the celestial sphere, combined with the requirements for accurate astronavigation indicate that the celestial tracking system should be capable of tracking second magnitude stars. This implies the detection of light power densities on the order of $10^{-12}$ watts/cm$^2$, the average incident power received from a second magnitude star in space.

Research commenced in 1959 and continuing at present has led to the development of sensitive photovoltaic visible and near infrared detectors. Sensitivity requirements and materials limitations have restricted usable devices to those with output impedances greater than one megohm. This high output impedance has placed typical cell time constants on the order of one millisecond or longer, and made signal sampling, through

light chopping, impossible at any usable frequency. The use of these photovoltaic cells in a servo system then appeared to require some form of impedance transformation.

As any tracking system must operate on a comparison basis and DC amplifier drift was found to be too great for system operation with inputs on the order of three microvolts (the output of a photovoltaic cell "seeing" a second magnitude star), it was decided to use chopping techniques. The slowly varying high impedance DC output of the photovoltaic sensors was to be converted by chopping and impedance transformation to a low impedance AC signal. Standard chopping techniques were found not space-compatible and they did not provide the required impedance transformation.

Research under AF Contract 33 (616) 6278 was concluded in 1962 with the development of manufacturing processes and design techniques to produce unipolar field effect transistors (Ref 4: ii). Devices submitted by the contractor had DC input impedances on the order of $10^{10}$ ohms. As the devices had low capacitance and a high $g_m$ coupled with output impedances as low as 10,000 ohms it appeared possible, using the unipolar transistor, to accomplish the impedance transformation and chopping functions during first stage amplification. The resulting circuitry was found space-compatible under space, weight, and radiation criteria.

After evaluating celestial tracking system functions, synthesis of a simple feedback loop was completed. Satisfactory results were achieved in the laboratory testing of system components and key assumptions were verified. The entire feedback loop for one axis control was tested in the laboratory, and, after difficulties with induced 60 cycle noise were overcome, the system tracked a source radiating light of similar spectral characteristics and power density to that of a second magnitude star in space.

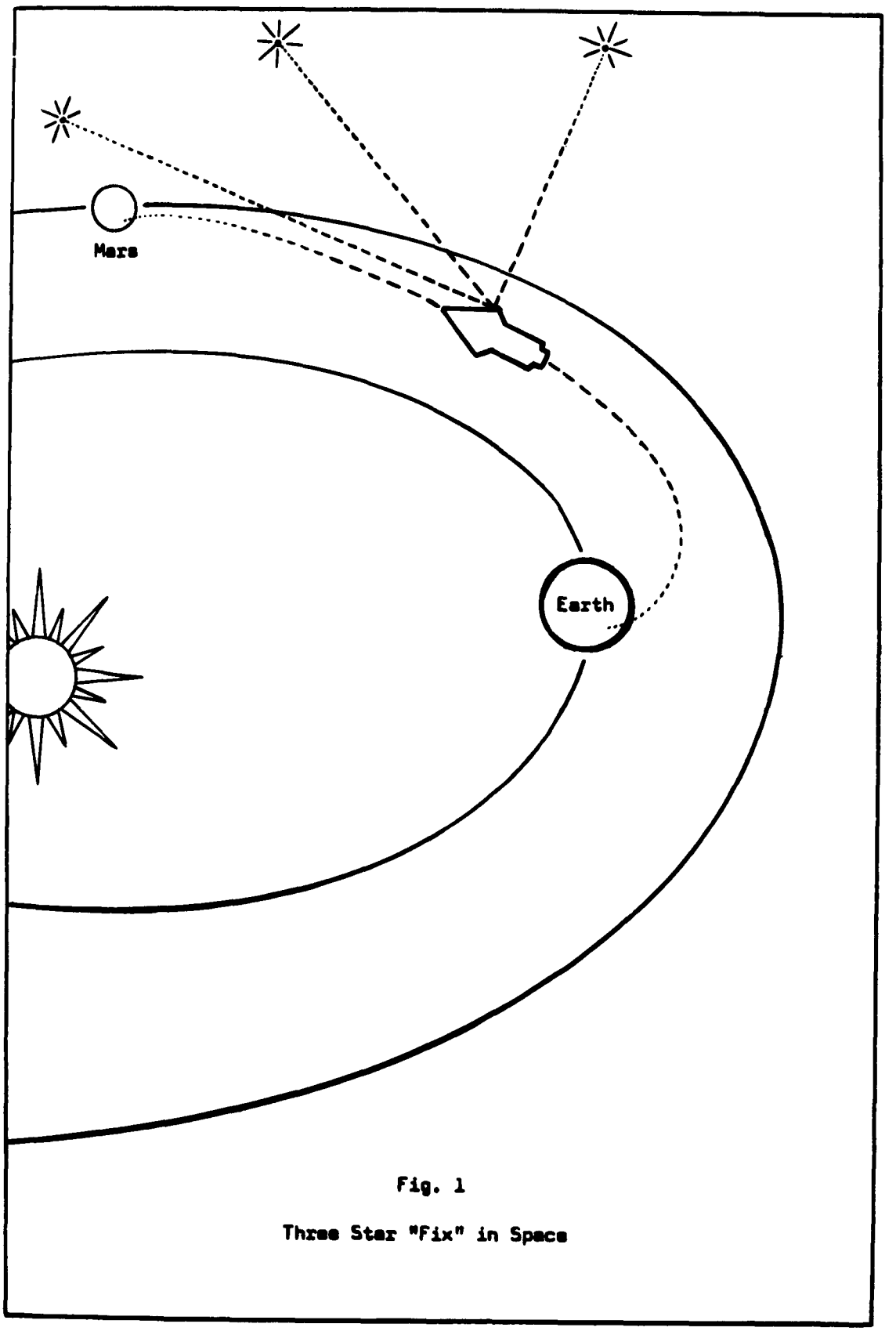


Fig. 1

Three Star "Fix" in Space

## II. Celestial Body Sensing And Tracking System Requirements

It will be assumed in this thesis that the satellite in which the celestial tracking system is to be used has been launched from earth, oriented in space, and satellite position with respect to the desired flight path relayed to the submicrominiaturized satellite computer. It is also assumed that tracking stations on earth have relayed to the satellite computer the expected angular positions of selected navigation stars with respect to the satellite coordinate system.

### Astronavigation

Navigation in space is similar to celestial navigation in an aircraft with the exception that a three dimensional fix must be obtained. A typical three star fix in space is shown in Figure 1. A unique position in space is determined when lines of position from three "fixed" stars are determined and the time of measurement is known accurately. Unlike terrestial navigation, celestial navigation in space is independant of a true horizon. If the angular measurements of the line of position of a star are accurately determined with respect to an arbitrary coordinate system, as shown in Figure 2, three such measurements, using three stars, will determine a unique point in space independant of the reference coordinate system. It should be noted that the stars used for a fix should be not less than 60 to 70 degrees apart on the celestial sphere (Ref 2: 17).

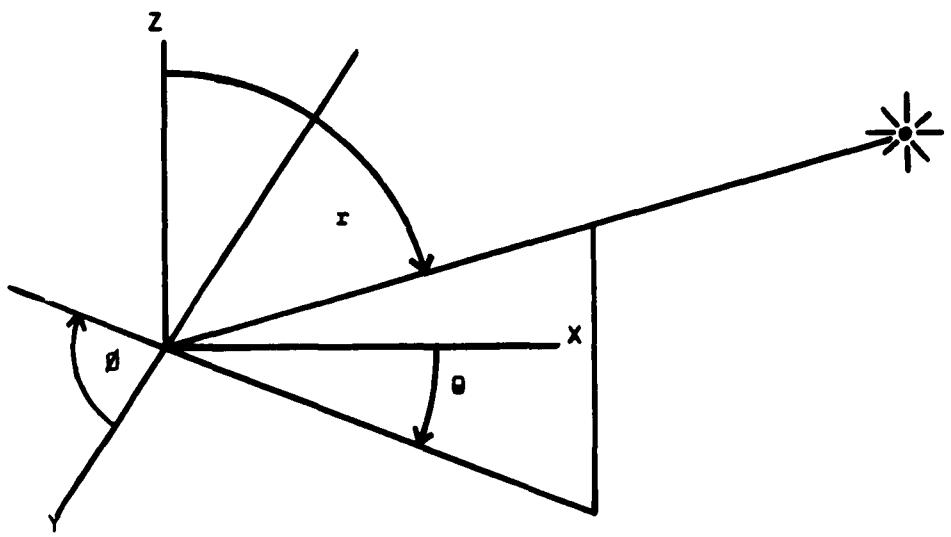


Fig. 2

Angular Measurement of Lines of Position

The positions of the common navigational stars on the celestial sphere were plotted to determine the required system sensitivity. As first and zero magnitude stars are not located in ideal positions for accurate navigation, and if the angles between stars selected for a fix are to be greater than 60 degrees, then the celestial tracking system should be able to track second magnitude stars.

## System Functions

Any system designed to be operated in space should be small in size, radiation resistant, of light weight and low power consumption, resistant to vibration, and possess a practical insensitivity to temperature changes. These considerations, plus the high degree of reliability required, can be called the criteria of space-compatability. Obviously space-compatability almost demands solid state, or better, molecular electronic circuitry.

In addition to being space-compatible, a celestial sensing and tracking system must perform the following functions:

1. Acquire a designated star.
2. Track that star continuously against a "no star" background.
3. Provide a readout of the angular bearing of the star, with reference to an arbitrary coordinate system, to a guidance device.

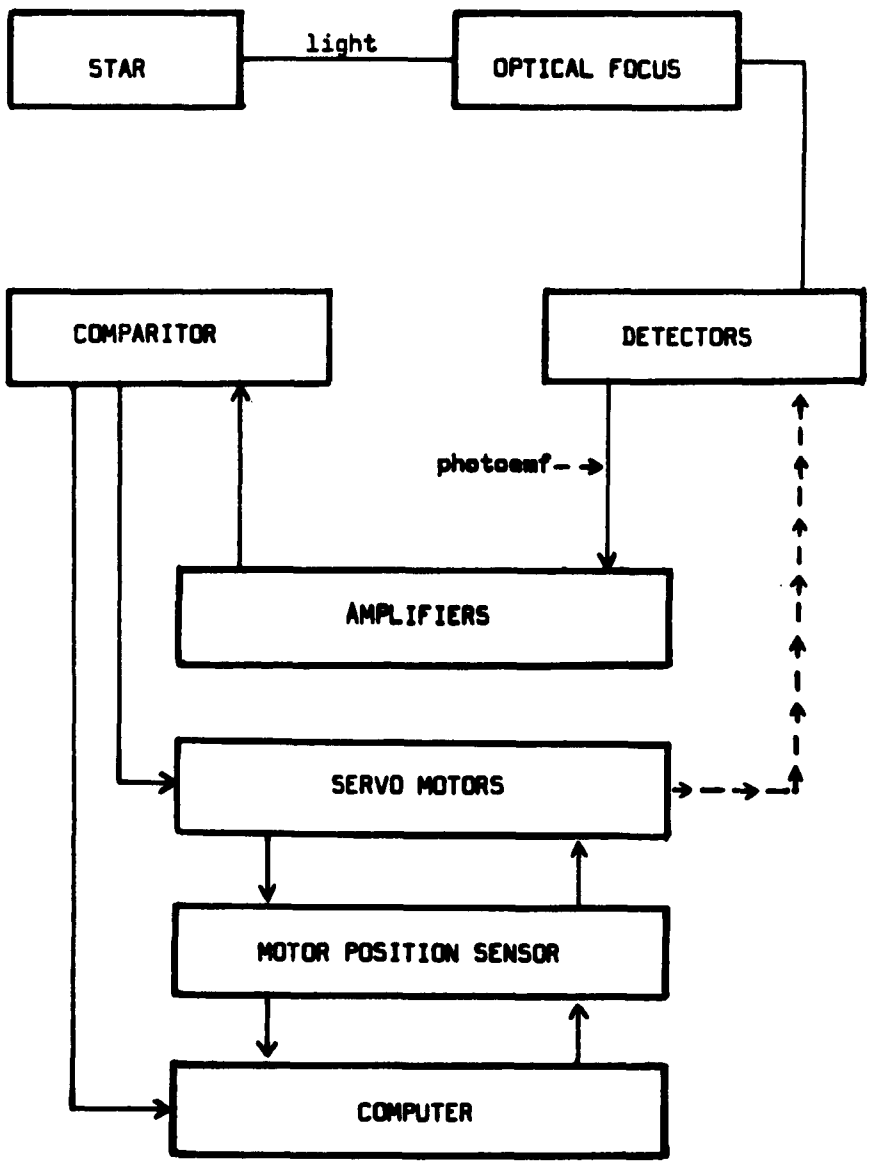


Fig. 3

Functional Block Diagram of a Star Tracking System

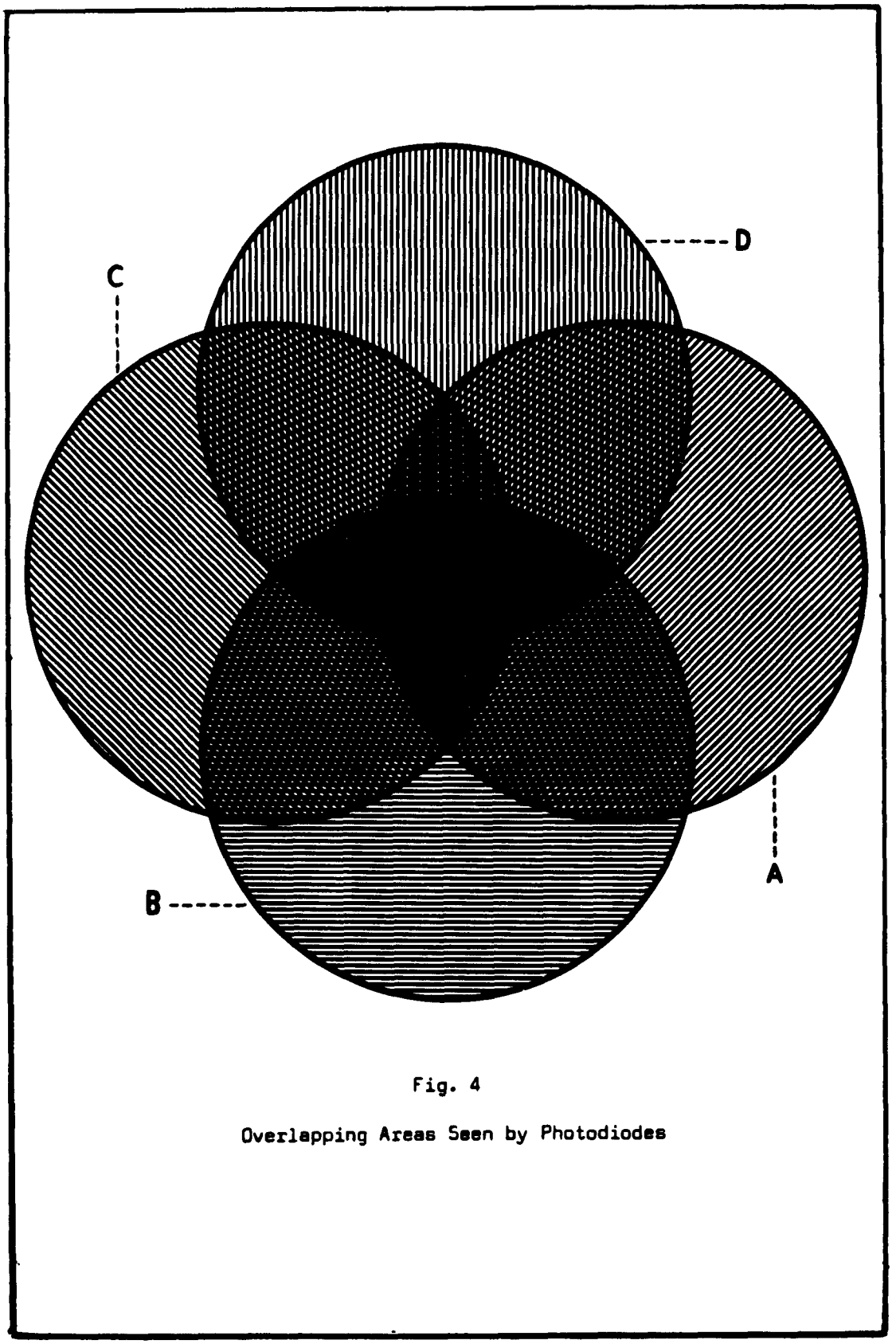


Fig. 4

Overlapping Areas Seen by Photodiodes

A possible functional diagram of the required system is shown in Figure 3. In the system of Figure 3, light from a selected navigation star is passed through two optical devices similar to telescopes. These devices limit the area on the celestial sphere which each detector sees, and provide an optical gain. To fulfill the star tracking function four detectors are needed, one pair for each axis or control channel, of the cartesian coordinate system. The optical devices are arranged as shown in Figure 4 so that the fields of vision of the devices overlap. Diodes D and B are an axial pair, as are A and C. Since the control channels for each axis are identical, the operation of only one channel will be discussed in this paper.

If light from the selected star is impacting upon one detector of a pair but not the other, then the voltage output of the two photovoltaic sensors or detectors will differ. As the photoemf output of the detectors is low, the voltage output of each is amplified independantly through a voltage gain of 1000. The separate voltages are then compared, and the servo motor controlling detector position along a coordinate axis is driven by the difference voltage until the difference vanishes. The star is then centered along that axis.

The system function of providing an angular readout of the selected stars position can be accomplished by a standard voltage divider arrangement. Since systems of this type were operational in 1944 and are fully covered in the literature

(Reference 7 for example), this function will not be further discussed in this paper.

The system function requiring acquisition of a designated star will be accomplished by using a computer program. When the satellite is oriented in space and its position along the programmed flight path is determined, each navigation star has an expected angular bearing with respect to the satellite coordinate system. Given this information the computer may, by generating appropriate voltages, drive the servomotors to the desired position. If neither detector "sees" the star after positioning, no photoemf will be generated. At this point the computer will drive the servomotors so as to start an "expanding square" area search. When a voltage differential is sensed at the comparator, the computer will cease sending search instructions and the sensing system will lock on to the star automatically. As the solution to this function is well known and its application, as outlined above, depends upon the specific servo equipment and computers installed, no further mention of this function will be made in this paper. The remainder of this thesis will be devoted to synthesis of a star tracking system.

Absolute System Sensitivity

In order to determine the absolute sensitivity required to detect a star of the second magnitude, it is necessary to calculate the energy density in watts/$cm^2$ received in space

from such a star. Assuming the color temperature of the star is the same as that of the sun, 5800 $^{o}K$ (Ref 5: 11), and noting that the power density of incident flux from the sun in space is 140 $mw/cm^2$ (Ref 20: 28), the incident flux from a second magnitude star in space is found to be approximately $6.3 \times 10^{-13}$ $watts/cm^2$. The incident flux is determined by using the formula $F_2 = \frac{F_1}{2.512^{M2 - M1}}$ (Ref 9: 74) where F is incident flux in $milliwatts/cm^2$, $M_1$ is the magnitude of the sun (-26.7), and $M_2$ is the magnitude of the star. If collecting optics with an optical gain of 20 are used (Ref 5: 12, Ref 15: 77), the total power on the detector at the focal point will be $1.26 \times 10^{-11}$ $watts/cm^2$. The star tracking system must be capable of detecting this low level of incident power on a comparison basis.

System Operation

If the celestial tracking system detectors, or photodiodes, are placed as shown in Figure 4, the output of the photodiodes will be a slowly varying DC voltage. Using the expected light power densities incident from second magnitude stars in space, the voltage differential between two detectors, one "seeing" the star and the other not, will be in the three microvolt range (As shown in Chapter III). This voltage must be amplified by a factor of $10^7$ (to 3 - 10 volts) before it can be used to

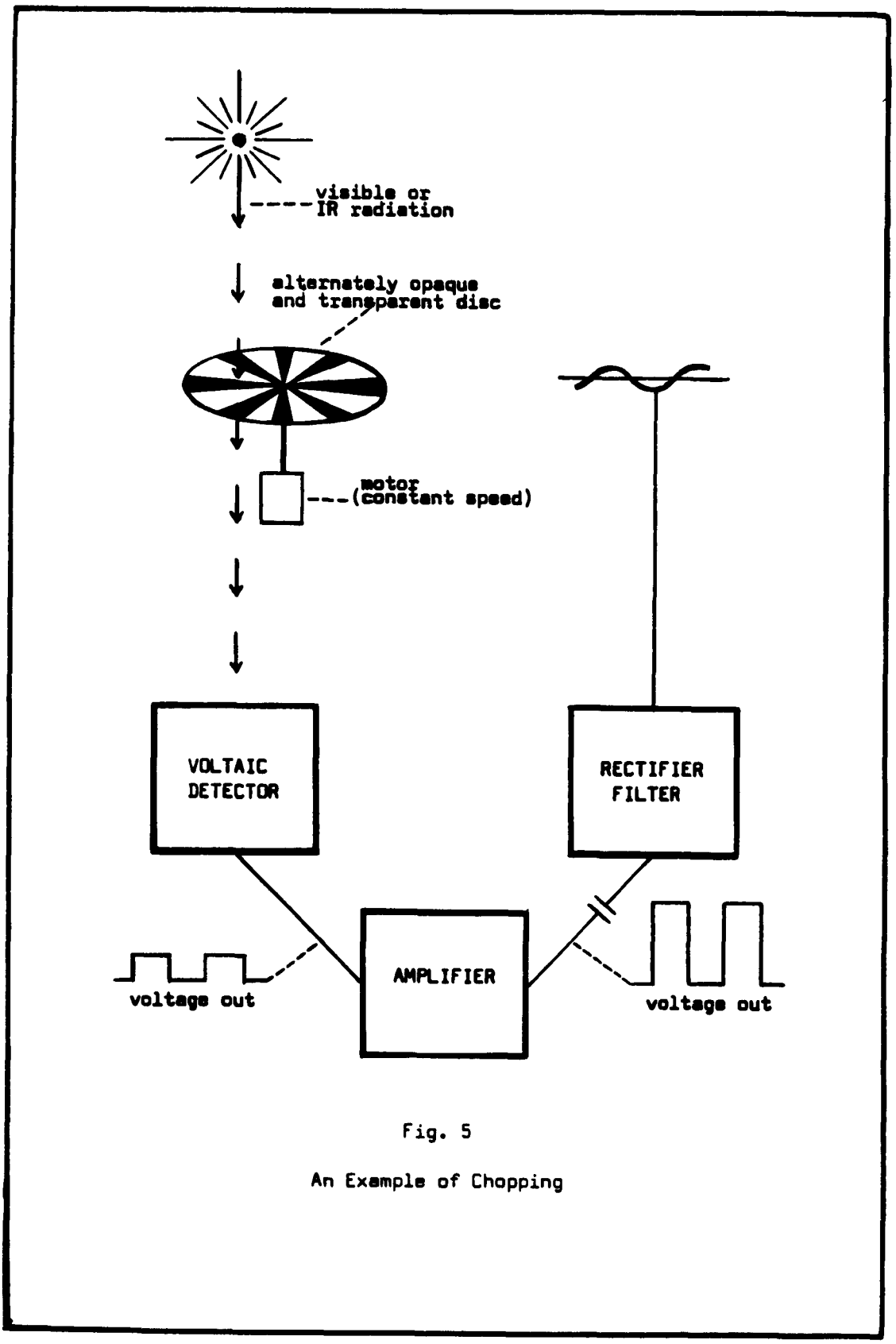


Fig. 5

An Example of Chopping

drive a servomotor. As the most stable DC amplifiers available have drift rates of 10 microvolts/hour or greater, even when placed in a temperature controlled environment, the amplification of a DC voltage differential in the three microvolt range is practically impossible if chopping techniques are not used (Ref 6: 495, Ref 8: 377, Ref 13: 453, Ref 17: 61, Ref 25: 39).

An example of a system using chopping techniques is shown in Figure 5 (Ref 10: 10). This system does not possess the required sensitivity, and the fragility of the disk and motor power requirements make it obviously unsuited for the space environment. Because of the space-compatability requirement, a lightweight, preferably electronic, version of a chopping system is required.

## III. Sensitive Photovoltaic Devices

### Theory of Operation

The theory of operation of a P-N junction photocell has been rigorously derived by Rittner (Ref 19). The theory may be summarized by noting that each incident photon of appropriate wavelength impinging upon the cell within a diffusion length of the junction lifts one electron from the valence band to the conduction band. The free electron-hole pairs thus created are swept across the P-N junction and appear as a reverse current. The magnitude of the reverse current is directly related, ignoring recombination at the junction, to the power density and wavelength of the impinging light. In the photovoltaic mode the photocell will act as a variable battery, with the output voltage directly proportional to the light incident upon the cell.

The magnitude of the junction recombination loss is small in a carefully designed cell, and may be made negligible by placing a large reverse bias across the P-N junction. The amount of bias allowed is severely limited by signal-to-noise considerations. With an optical gain of 20, the power density expected from a second magnitude star, $1.26 \times 10^{-11}$ watts/cm$^2$, corresponds to a photon density of $14.2 \times 10^{6}$ photons/cm$^2$-sec (Ref 5: 29), or a maximum possible photocurrent of $2.4 \times 10^{-12}$ amperes (Ref 22: 9). A simple statistical calculation shows that a current of $4.5 \times 10^{-7}$ amperes will have an RMS fluctuation

Table I

Characteristics of the GAU 401

Test Conditions

| | |
|---|---|
| Blackbody Temperature | 1200 $^{o}K$ |
| Chopping Frequency | 400 cps |
| Bandwidth | 4 cps |
| Cell Temperature | 25 $^{o}C$ |
| Load Resistance | 10 megohm |
| Load Capacitance | 250 pf |

Electrical Characteristics

| | | |
|---|---|---|
| Area | 1.0 | $mm^2$ |
| NEP | $8 \times 10^{-10}$ | watts |
| Position of Spectral Peak | 0.85 | microns |
| NEP (at spectral peak) | $5 \times 10^{-13}$ | watts |
| Cell Impedance | 1.5 | megohm |
| Cell Capacitance | 350 | picofarad |
| Cell Time Constant | 1.0 | millisecond |
| Cell Response to 2780 $^{o}K$ Blackbody Radiation | 0.03 | microamp/microwatt |
| Noise Equivalent Lumens | $7 \times 10^{-11}$ | lumens |

Note

NEP is defined as:

$$\text{NEP (watts)} = \frac{\Phi A}{S/N}$$

where: $\Phi$ = Power density at plane of cell in watts/$cm^2$
A = Active cell area in $cm^2$
S = Signal in microvolts
N = Noise in microvolts

For a cell area of 4.0 $mm^2$

| | | |
|---|---|---|
| NEP | $1.17 \times 10^{-9}$ | watts |
| Noise Equivalent Lumens | $12.1 \times 10^{-11}$ | lumens |

(From Ref 18: 1)

of $3.8 \times 10^{-13}$ amperes (Ref 22: 10). In the photovoltaic operation of a P-N junction, this value of $4.5 \times 10^{-7}$ amperes gives an upper limit for the saturation current $I_o$ if signal-to-noise ratio is considered.

According to diode theory, the operating impedance of a P-N junction will be equal to $KT/qI_o$ near the zero bias point (Ref 19: 21). Here K is Boltzmanns' constant, T is absolute temperature, q the electron charge, and $I_o$ the reverse saturation current. Substitution of the desired maximum $I_o$ value into the above formula for room temperature yields a junction resistance $R_j$ of 500,000 ohms. If the signal-to-noise ratio is to be increased, $I_o$ must be decreased and $R_j$ increased. Additionally, if the junction is to be the major source of noise in the system, the load resistance $R_l$ should be much greater than the junction impedance. From the above considerations then, the photovoltaic cell should be at or near zero bias.

## Characteristics of Available Photovoltaic Devices

Table I lists the characteristics of the GAU 401 visible detector (photodiode). This device, made of gallium arsenide, is the most sensitive presently available. Final device specifications may vary as it is still in the experimental stage. Presently available silicon photodiodes are not usable at the required system sensitivities. When used as photovoltaic sensors they are noise limited as they require a relatively large bias current for effective operation.

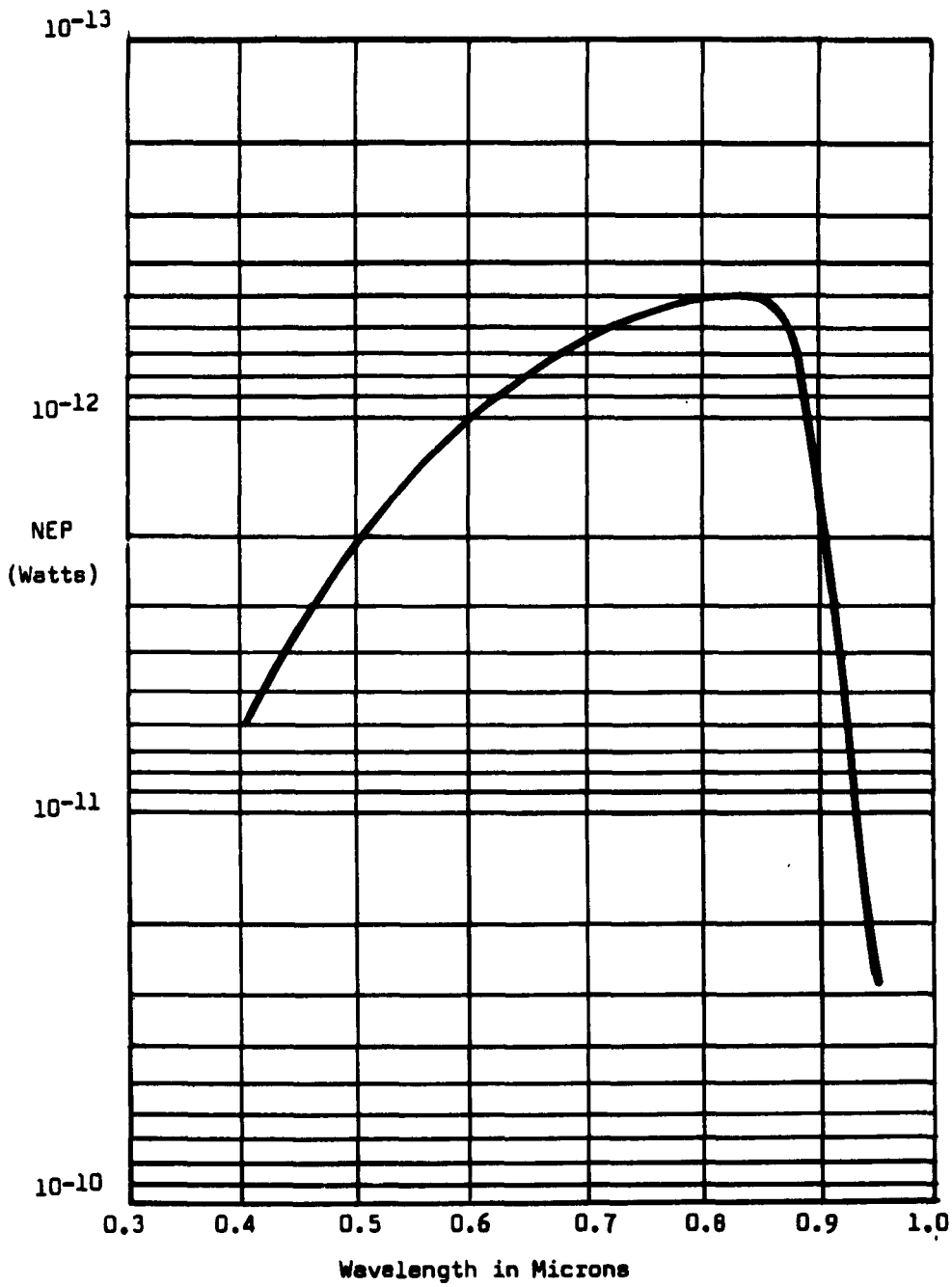


Fig. 6

Typical Spectral Response of the GAU 401

(From Ref 18: 2)

Figure 6 shows the relative spectral response of the GAU 401 to visible and near infrared radiation. It may be noted that the signal output will not vary appreciably with the color temperature of the star as the GAU 401 is primarily a visible sensor and a star is classed by magnitude according to its light power output in the visible range.

Use in a Tracking System

If two identical GAU 401 photodiodes were used as single axis sensors in the configuration of Figure 4, one devices "seeing" a second magnitude star and the other not, the DC voltage differential between the two devices could be expected to approach 3.78 microvolts. (Cell response of 0.03 microamp/microwatt across $10^7$ ohms times incident power of $1.26 \times 10^{-5}$ microwatts if an optical gain of 20 is assumed.) If both photodiodes were "seeing" the star at one instant, the movement of the satellite carrier on its programmed flight path would make the star image appear to drift across the face of the optical devices, causing a slowly increasing DC differential voltage.

To be useful this three microvolt maximum output must be amplified by a factor of $10^7$. As previously stated, DC amplification is not possible at these low signal levels. The photodiode, the only device sensitive enough for use in tracking, has a cell time constant too long to allow chopping at any reasonable frequency. In addition, the photodiode

internal impedance and required load resistance are too high to be compatible with normal transistor circuitry, and the cell must be kept at near zero bias.

The preamplifier of any system using these cells must have an input impedance in the megohm range, be capable of electronic chopping, provide an impedance transformation of $10^{-5}$, supply a noise free voltage gain of $10^{3}$, and be space-compatible. These extremely stringent requirements are met by the recently developed, but still experimental, unipolar field effect transistor.

# IV. The Unipolar Transistor

## Characteristics

The unipolar transistor is a voltage controlled transistor analogue of the vacuum triode. It is so named because device operation depends essentially on the presence of majority carriers. Because of this fact it has a higher resistance to radiation than bipolar transistors (Ref 4: 46). The structure of the unipolar transistor is illustrated in Figure 7, and the equivalent circuit is shown in Figure 8. In simplest form the device consists of a semiconductor single crystal with two P-N junctions positioned between two ohmic contacts as shown. In operation, the conductivity of the current path between the ohmic contacts is modulated by application of a transverse electric field via the P-N junctions. The regions of the device are descriptively designated as source and drain (ohmic contacts), gates (P-N junctions), and channel. The channel is the region located between the opposing gate junctions. The typical device employs an N type channel to utilize the higher mobilities of the current carrying electrons and therefore requires a negative source-to-drain voltage for proper operation.

Figure 9 shows the volt-ampere characteristics of the unipolar transistors (designated X - 1 through X - 4 for convenience) used in laboratory testing of the circuits shown

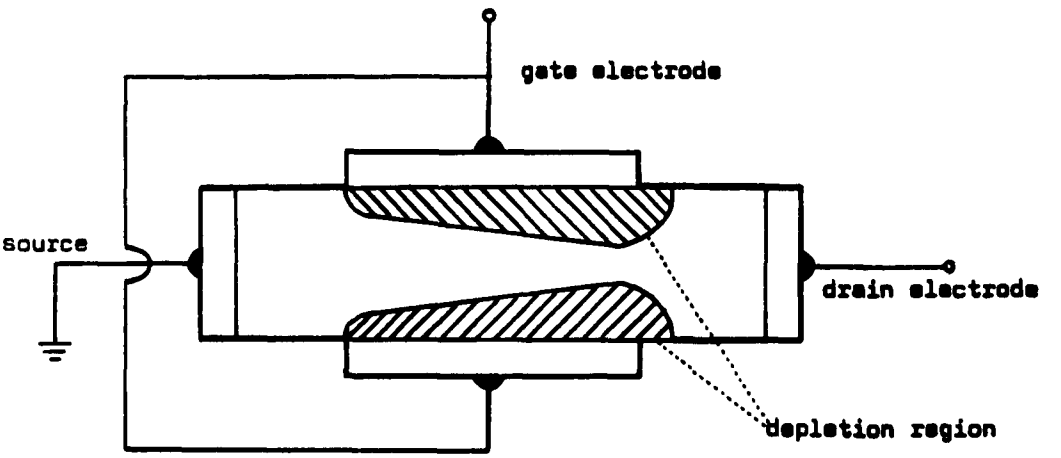


Fig. 7

Unipolar Transistor Structure

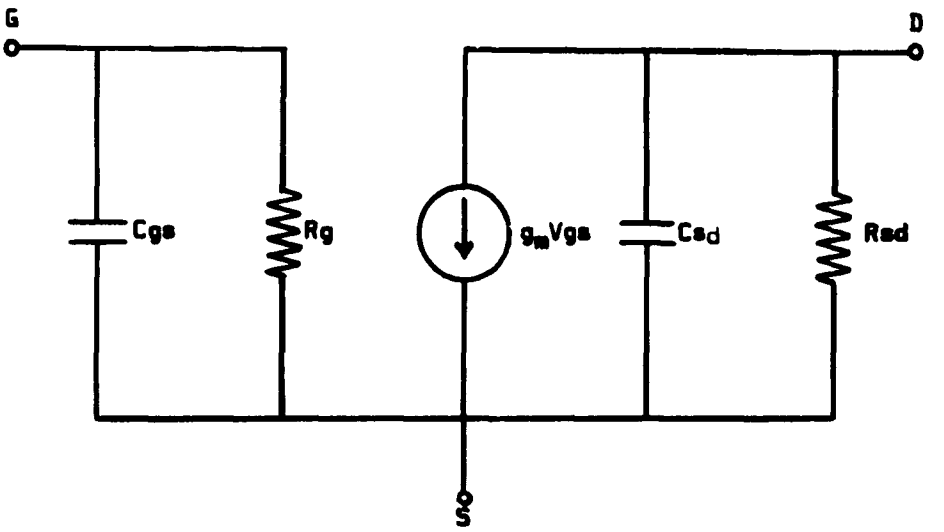


Fig. 8

Unipolar Transistor Equivalent Circuit

(From Ref 4: 3)

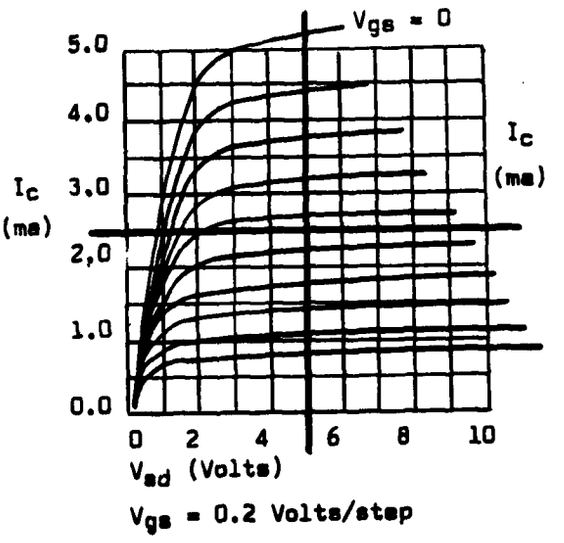


X - 1

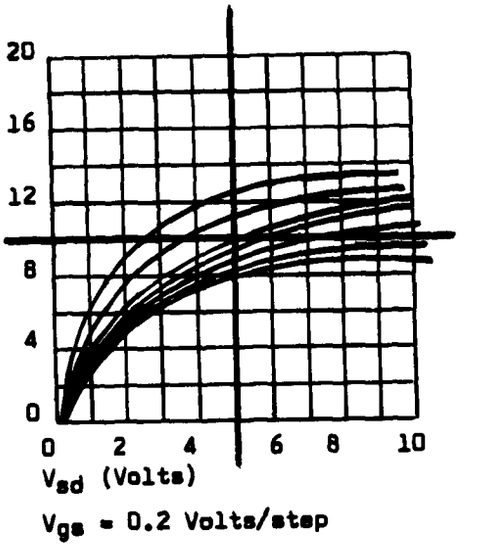


X - 3

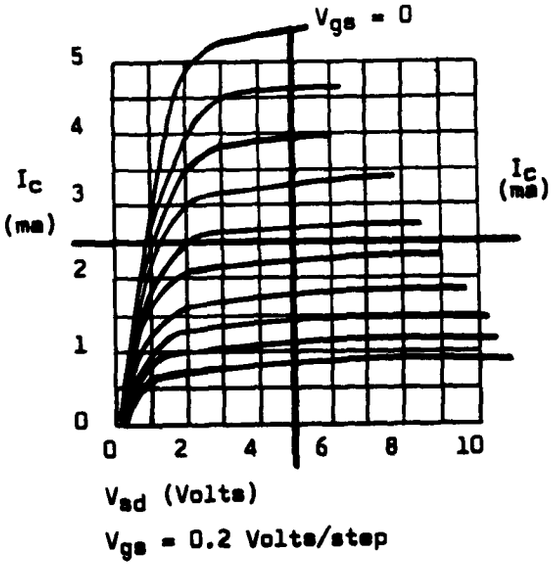


X - 2

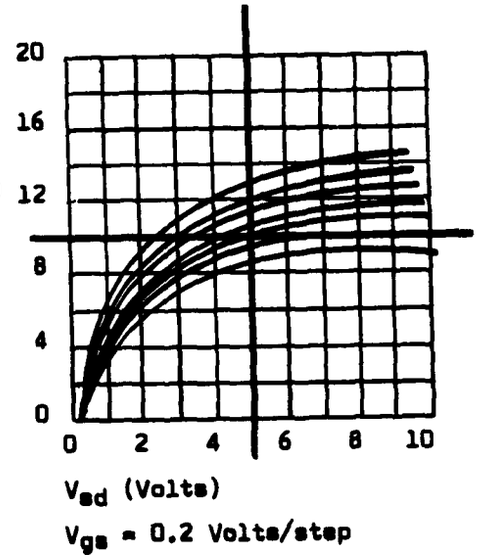


X - 4

Fig. 9

Unipolar Transistor Volt-Ampere Characteristics
for Units X - 1, X - 2, X - 3, and X - 4

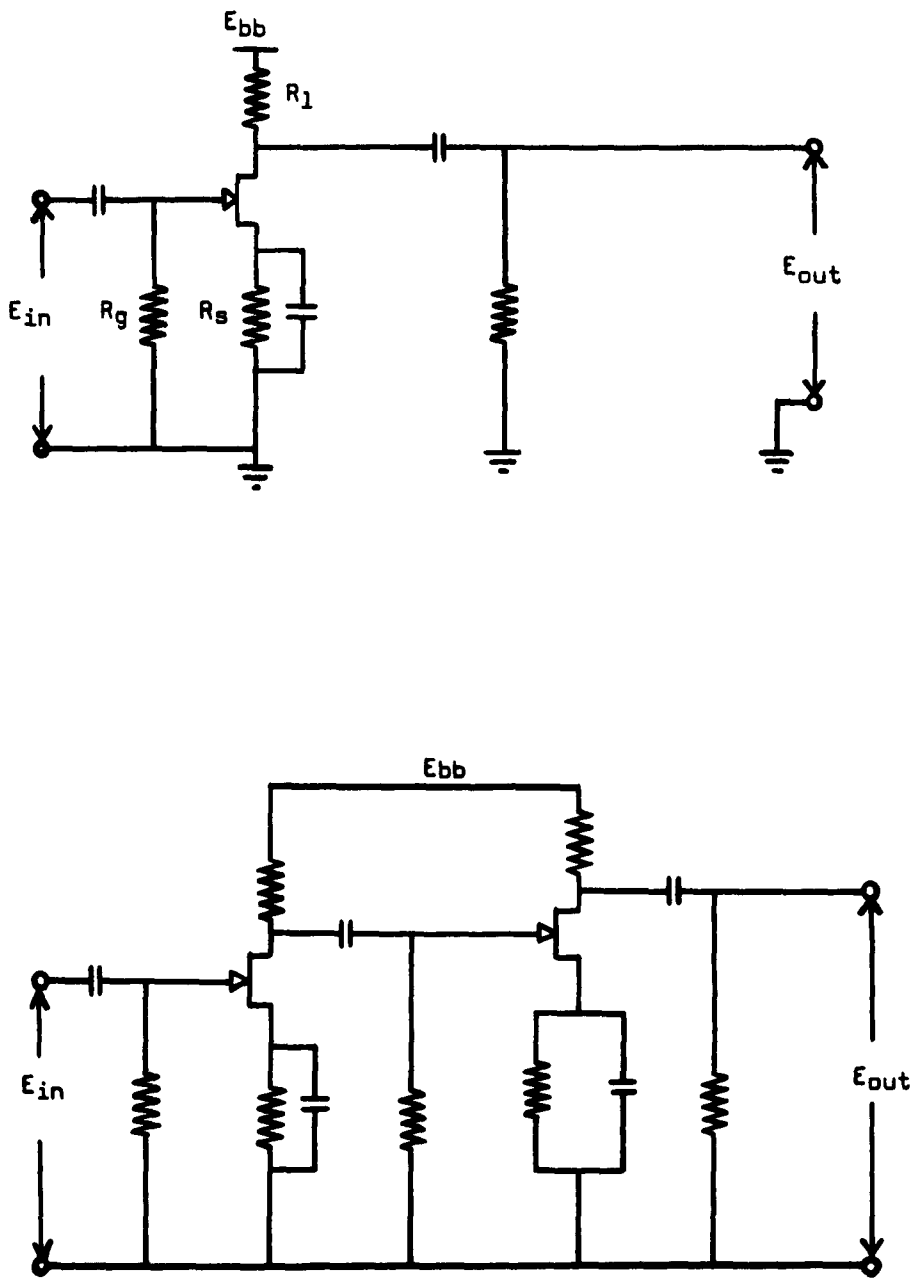


Fig. 10

Typical High Gain Unipolar Transistor Amplifiers

(From Ref 4: 42)

in this thesis. The device characteristics were obtained using a Techtronix Transistor Curve Tracer. Actual transistor characteristics, i.e., channel current, differed by a factor of 100 from the manufacturers published specifications in the case of the X - 2.

Use as an Amplifier

The unipolar transistor is an inherantly low noise device. For audio frequency amplification the AC parameters of the device do not differ appreciably from the DC parameters (Ref 4: 13), typical values of which are shown in Table II.

Table II

DC Parameters of Units X - 3 and X - 4

| Parameter | Unit X - 3 | Unit X - 4 | Units |
|---|---|---|---|
| Cutoff $V_g$ | -1.8 | -3.5 | Volts |
| Small Signal $g_m$ | 2000 | 6000 | Micromhos |
| Large Signal $g_m$ | 1000 | 4500 | Micromhos |
| Pinch Off ($W_o$) | 2 | 5 | Volts |
| $I_{do}$ | 1.8 | 16 | Milliamps |
| $C_{gs}$ | 15 | 15 | Picofarads |
| DC Input Impedance | 50,000 | 50,000 | Megohms |
| Maximum $V_{gd}$ | 20 | 20 | Volts |

When used as an amplifier the small signal voltage gain of the unipolar transistor may be computed using the equivalent circuit of Figure 8. Using parameters taken from the volt-ampere characteristic of device X - 1, Figure 9, i.e., $g_m$ = 3200 micromhos, channel resistance $R_d$ = 40 Kohm, and using a load resistance $R_l$ of 100 Kohm, the voltage gain $G = \frac{g_m R_l R_d}{R_d + R_l} = 92$. In testing the

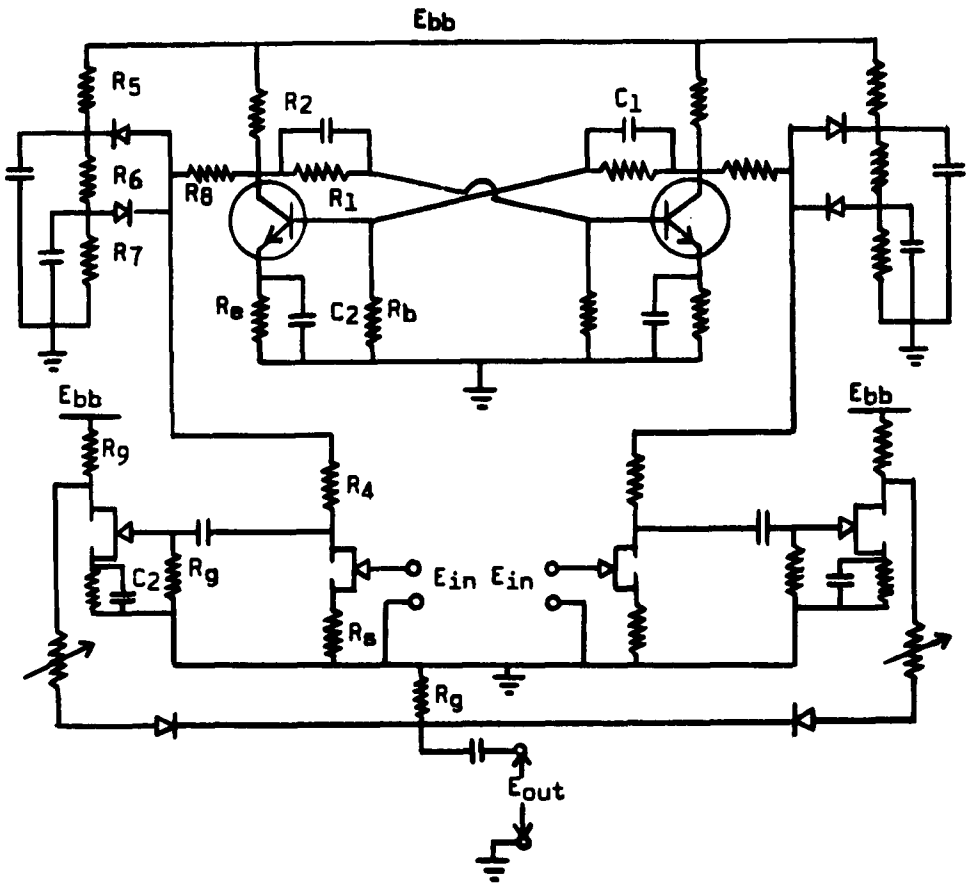


| | | | |
|---|---|---|---|
| $R_e$ = 560 | ohm | $C_1$ = 0.366 | mfd |
| $R_b$ = 5.6 | Kohm | $C_2$ = 1 | mfd |
| $R_1$ = 15 | Kohm | Unmarked = 50 | mfd |
| $R_2$ = 1.5 | Kohm | Diodes 1N315 | |
| $R_s$ = 4.7 | Kohm | Transistors 2N343 | |
| $R_4$ = 47 | Kohm | Unipolar Transistors FSP 400 | |
| $R_5$ = 10,630 | ohm | | |
| $R_6$ = 560 | ohm | | |
| $R_7$ = 11,120 | ohm | | |
| $R_8$ = 18 | Kohm | | |
| $R_9$ = 68 | Kohm | | |
| $R_g$ = 500 | Kohm | | |

Fig. 11

High Gain Two Channel
Differential DC Chopper Amplifier

X - 1 inserted in the circuit of Figure 10 gave a small signal gain of 98 with $R_1$ = 107 Kohm and $E_{bb}$ = 100 volts. As a high $E_{bb}$ is difficult to obtain in missile or satellite applications, 60 volts was chosen as a standard $E_{bb}$ for circuit synthesis. Device X - 2 gave a voltage gain of 58 with $R_1$ = 68 Kohm, $R_s$ = 4.7 Kohm, and $E_{bb}$ = 60 volts in the circuit of Figure 10.

Electronic Chopping

There are two convenient methods of chopping available using the unipolar transistor. The first and simplest method is to drive the gates of a unipolar transistor with a square wave to turn the device alternately on and off. This method is not usable with the GAU 401 because of the long cell time constant. In addition signal-to-noise considerations, as discussed in Chapter III, require the photodiode to be at or near zero bias.

Figure 11 shows the method of electronic chopping selected for this project and tested in the laboratory. The output of the multivibrator is 30 volts DC plus a 30 volt superimposed square wave. The diode clipping circuits stabilize this output to 30 volts DC with a 400 cycle 1.5 volt very square wave superimposed. The first stage gates are essentially at ground level and, as there is no bypass capacitor on the first stage source resistors, $R_s$, the gate-to-source voltage varies with the driving square wave.

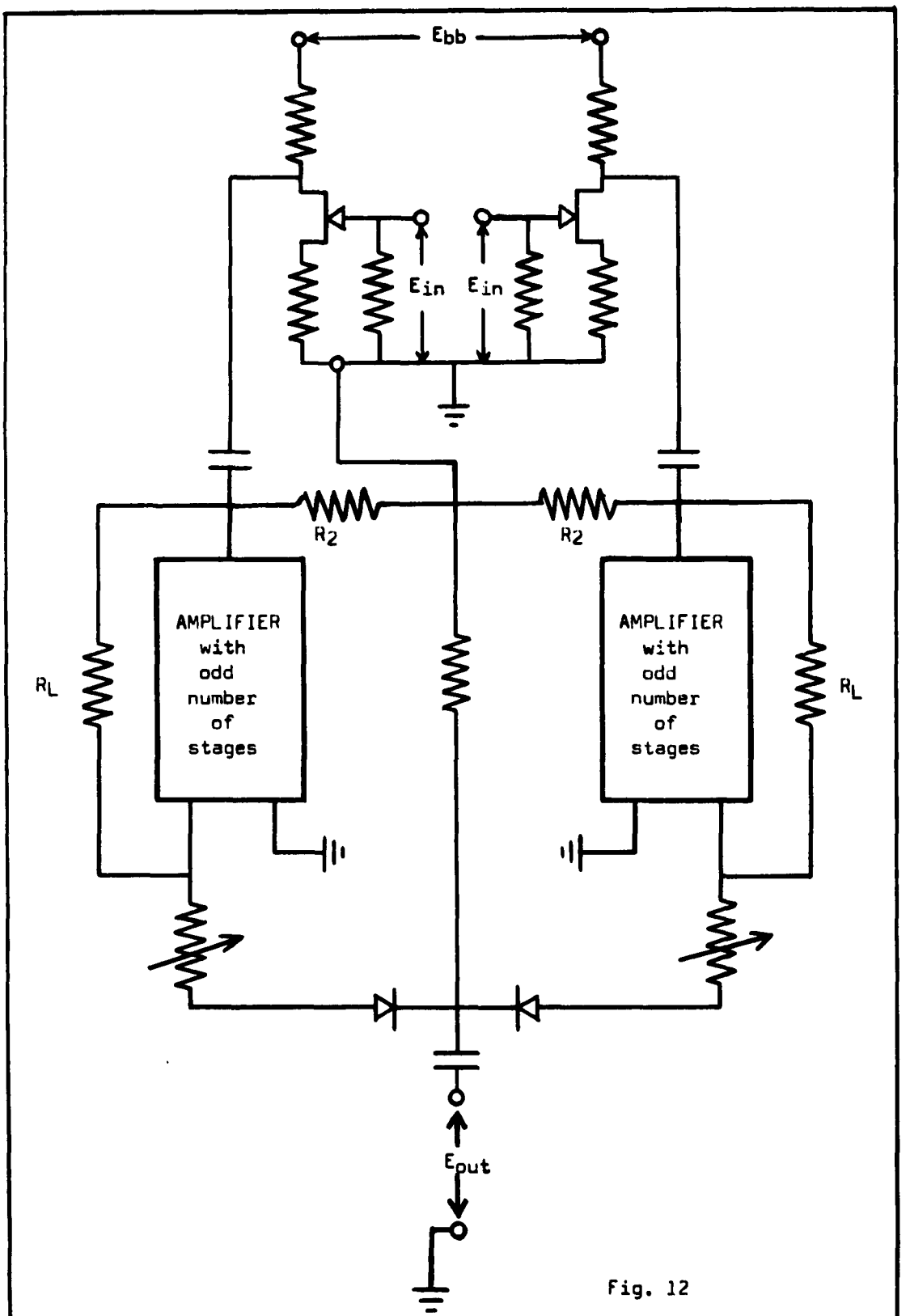


Fig. 12

Amplifier Gain Stabilization

The magnitude of this variation is $\frac{R_s E}{R_s + R_4 + R_d}$ equal to $\frac{(4.7K)(1.5)}{61.7K}$ = 0.114 volts. An increase in source voltage is the same as a decrease in gate voltage in its effect on the device. When $E_{bb}$ increases, $V_{gs}$ increases and $E_o$ increases. At the second stage $V_{gs}$ decreases and $E_o$ decreases. The second stage device may even saturate. When $E_{bb}$ returns to 30 volts, $E_o$ of the second stage increases and that channel conducts through the diodes. The absolute value of the gate voltage with respect to ground is determined by the amount of light falling on the photodiode. Figure 15 illustrates the placement of the photodiodes in the circuit. In this configuration the changing source-to-ground voltage has a negligible effect on the photocells.

When unipolar transistors were placed in cascade as shown in Figure 10, very low noise small signal gains of 2600 were realized. If a third stage were added and feedback techniques applied as shown in Figure 12, the amplifier gain could be strongly stabilized at 1000 with $G = \frac{R_L}{R_L + R_2}$. This usage would eliminate requirements for matched devices in the purely amplifying stages and improve system stability. As sufficient unipolar transistors were not available to build a pair of feedback amplifiers as indicated in Figure 12 and the use of unipolar transistors was indicated by noise considerations, the circuit of Figure 11 was used in optical and noise testing.

Use as an Impedance Transformer

If $E_{bb}$ and $R_1$ (and consequently gain) are lowered in the circuit of Figure 10, the unipolar transistor may be used as an impedance converter. When the X - 3 was inserted in the circuit of Figure 10 with $E_{bb}$ = 20 volts and $R_1$ = 22 Kohm, an impedance transformation ratio of $3 \times 10^{-2}$ and a voltage gain of 10 were realized. Though the unipolar transistor is not suitable for high power levels (Ref 4: 38), it is particularly attractive for transforming high impedance inputs at low power levels.

# V. 400 Cycle Servo Motors and Power Amplifiers

## Torque-Voltage Characteristics

The typical torque-voltage characteristic of a 400 cycle servo motor is shown in Figure 13. The zero torque range is of particular interest in that a continuous voltage may be applied to the field coils and no motor rotation will occur if a specific driving voltage is not present.

## Servo Motor Operation

If a single phase 400 cycle AC servo motor is used in each axis to control the movement of the detectors, the direction of motor rotation must be controlled by the direction of the error. The direction of motor rotation can be controlled by the phase relationship of the voltages applied to the field coils and armature. If the voltages are in phase the motor will rotate in one direction. If the phase of the two voltages can be made to differ by $180^{o}$, the motor will reverse its direction of rotation.

## Solid State Servo Power Amplifiers

The mechanics of servo amplifier design are well covered in the literature. An adequate solid state servo power amplifier, taken from Reference 24: 176, is shown in Figure 14. The pre-amplifier stage was built and tested for impedance matching in conjunction with the circuit of Figure 15.

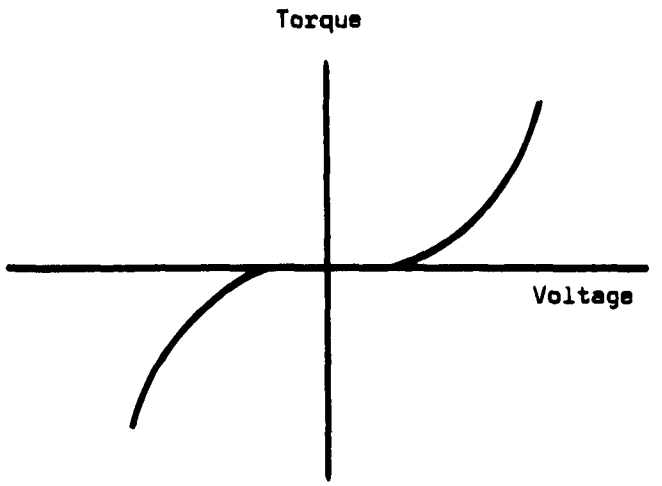


Fig. 13

Typical 400 Cycle Servo Motor Torque Characteristics

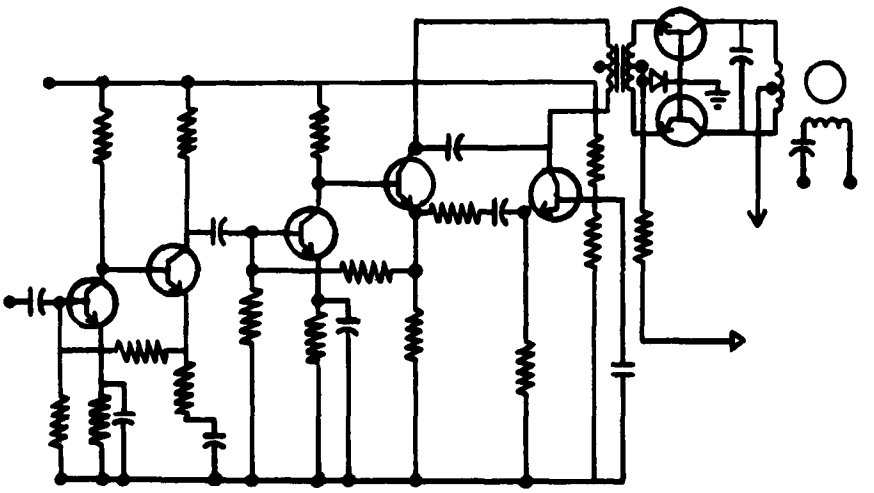

Fig. 14

A Solid State
400 Cycle Servo Amplifier

(From Ref 24: 176)

# VI. Circuit Synthesis

## Component Requirements

Matched photodiodes are required for best operation of the star tracking system. If the outputs of the two devices vary significantly, some compensation may be achieved by varying the load resistance seen by the diodes. As photovoltaic output is not necessarily linear over the useful light input range of the devices and may vary with temperature, this compensation will be accurate only for a specific range of light inputs and temperature conditions. The method of inserting the photodiodes into the tracking circuitry is shown in Figure 15. This isolation of the photodiodes was used because of the signal-to-noise considerations discussed in Chapter III.

If a pair of matched unipolar transistors is used in the chopping stages and amplifier gain stabilization, as discussed in Chapter IV, is employed in the succeeding purely amplifying stages, the voltage gain of each channel will remain fixed over a fairly wide signal range and temperature variation. This ideal circuit could not be tested because sufficient unipolar transistors were not available. The circuit of Figure 15 was tested using approximately matched pairs of unipolar transistors similar to Units X - 1 and X - 2.

The 1N315 diodes required in Figure 15 should be as closely matched as practicable. The use of trimmer resistances,

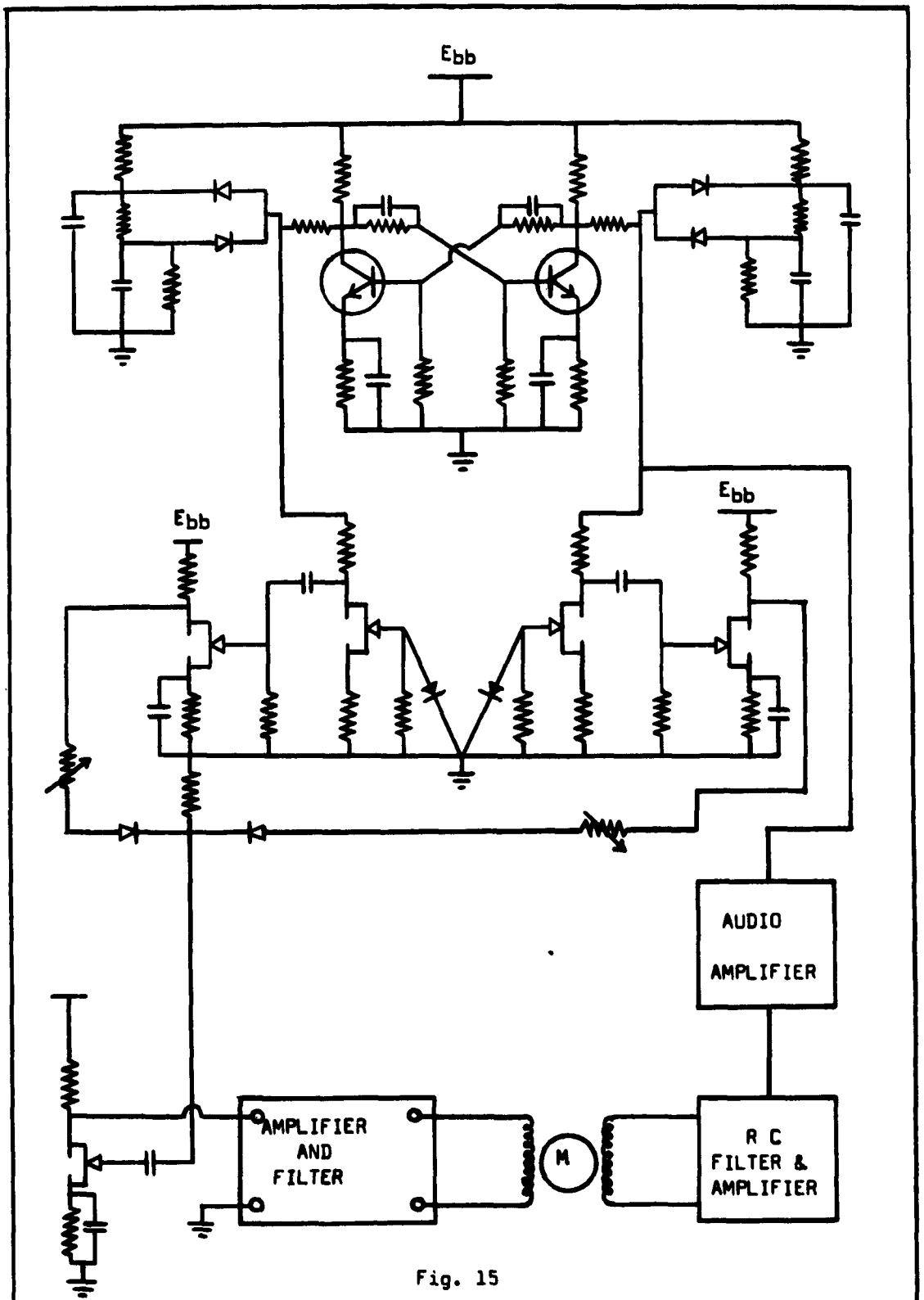


Fig. 15

Complete One Axis Star Tracking Circuitry

as shown, compensate for mismatch over a limited temperature range.

The 2N343 transistors required for the multivibrator of Figure 15 need not be closely matched. All resistors in the preamplifier circuitry should be accurate to at least one percent. The trimmer resistances can be used to peak the circuits.

## Circuit Operation

Figure 15 shows the complete impedance transformation, chopping, and preamplification circuitry for one axis of the star tracking system. The circuit operation can perhaps be best understood by following the one axis functional block diagram and associated waveforms of Figure 16.

When the trimmer resistances are properly adjusted and the photodiodes are exposed to identical light power densities, the only AC system output will be the 400 cycle reference phase delivered to the field coils of the servo motor from one side of the multivibrator. A negligible 400 cycle component is contained in the essentially DC output of the comparitor or summer at this time.

If the light power density to which one photodiode is exposed differs significantly ($1.26 \times 10^{-11}$ watts/cm$^2$) from the original value, the gate bias of the first stage of the preamplifier of one channel will change by 3.5 microvolts. If the voltage gain of the preamplifiers is stabilized at

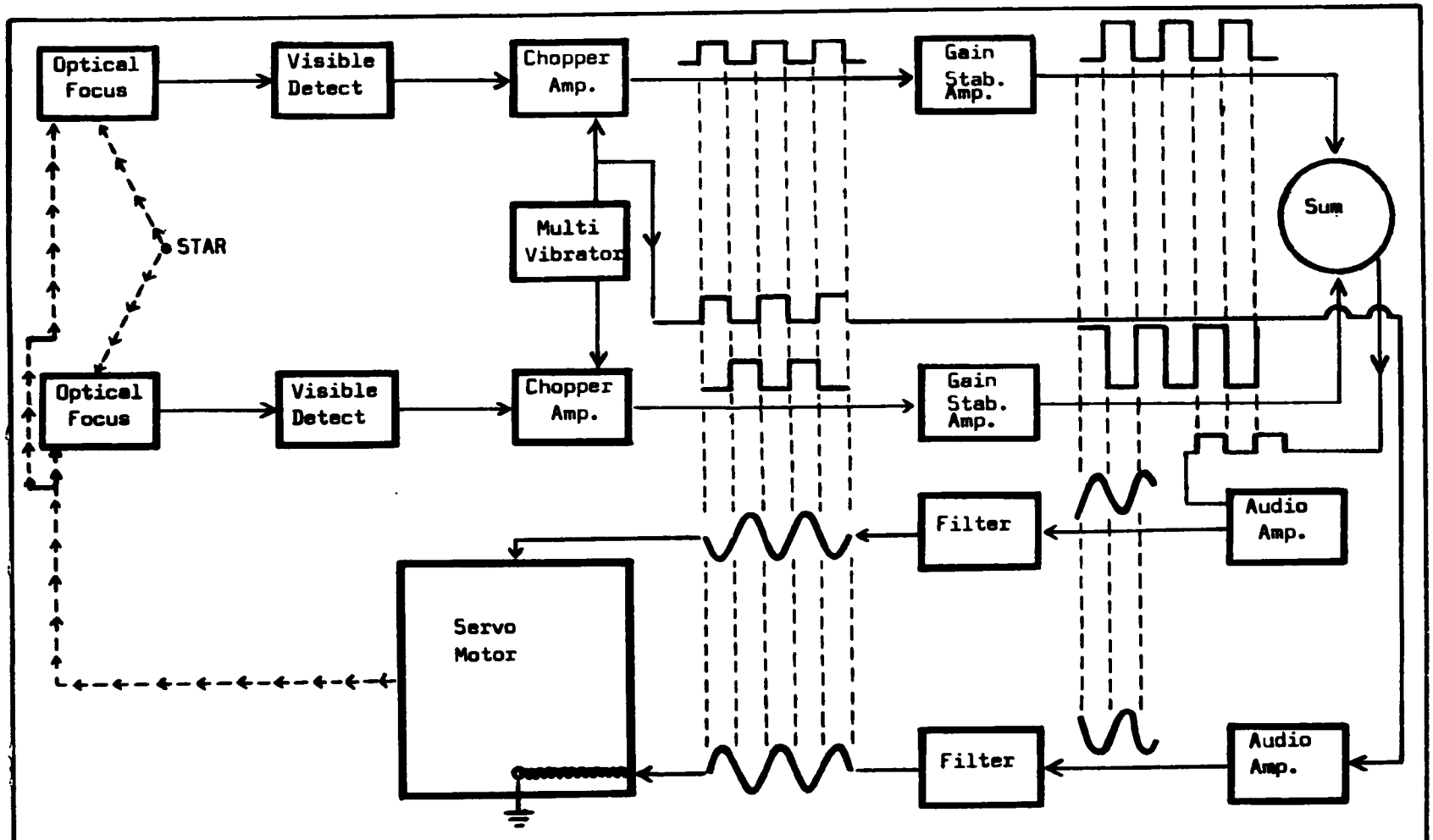


Fig. 16

A One Axis Functional Block Diagram of the Star Tracking System

1000, this DC differential will appear as a square wave at the summer with a valley to peak amplitude of 3.5 millivolts. If the impedance transformer stage has a voltage gain of 10, the magnitude of the 400 cycle component of the square wave will be 22.2 millivolts. The phase of the 400 cycle component will reflect the direction of error, being either in phase or 180° out of phase when compared to the 400 cycle voltage applied to the field coils of the servo motor. The 400 cycle error voltage will control the direction of rotation when applied to the armature of the servo motor. A Fourier analysis of the system waveforms (Appendix A) shows that the magnitude of the 400 cycle component of the square wave output of the summer will be related to the magnitude of the differential DC voltage (E) of the photodiodes by a factor of 2EG/pi where G is the gain of the preamplifier.

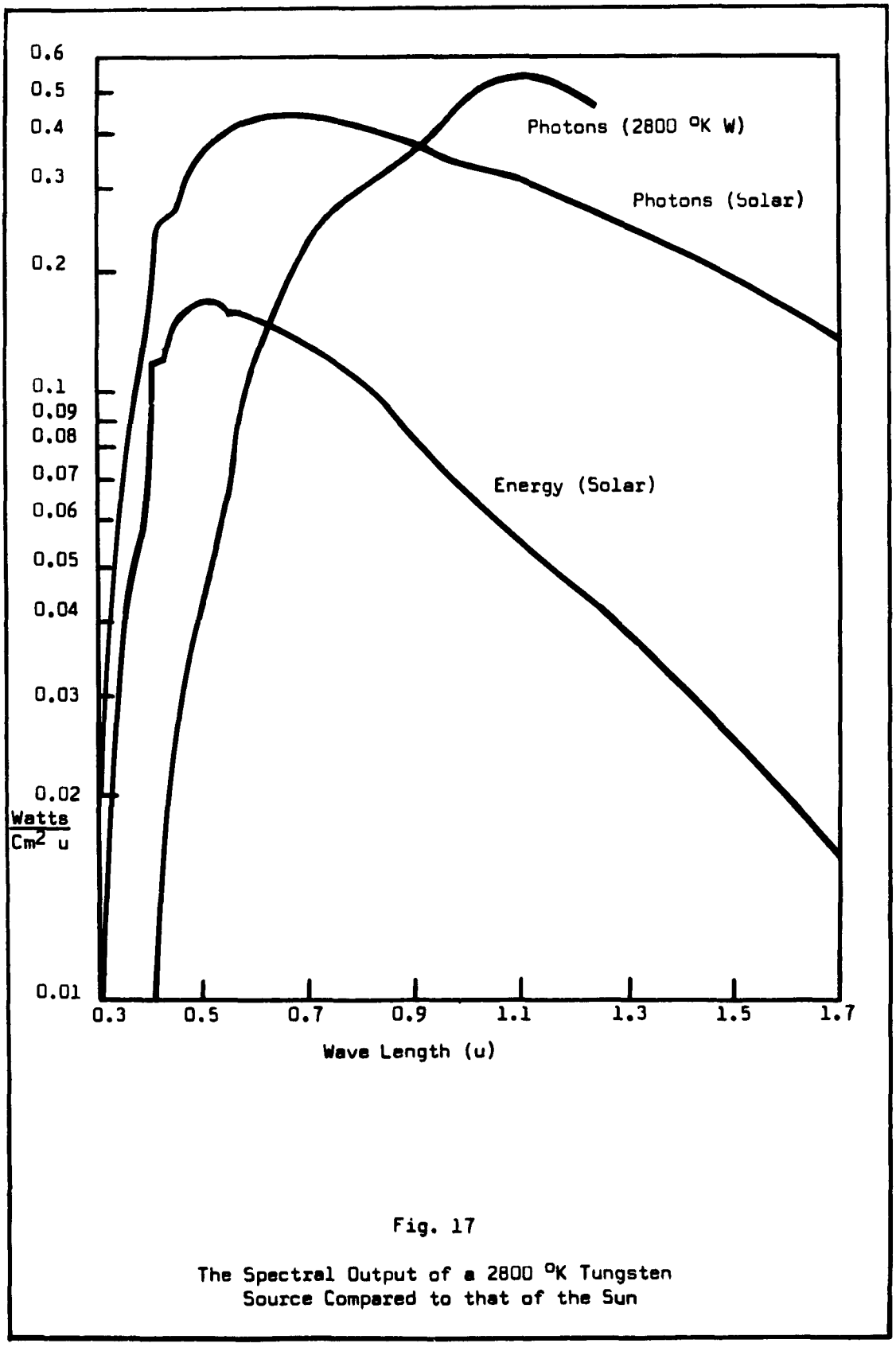


Fig. 17

The Spectral Output of a 2800 °K Tungsten Source Compared to that of the Sun

# VII. Experimental Equipment

## Optical Equipment

A light source of similar spectral characteristics and incident power output to a second magnitude star was required to accurately evaluate the performance of the star tracking system. Calibrated light sources of 2800 $^{o}K$ tungsten were used for this purpose. Figure 17 shows the spectral output of a 2800 $^{o}K$ tungsten source compared to that of the sun. The particular source used had a calibrated output of 26.3 lumens. By placing the test diode at a distance of 178 centimeters from the light source and decreasing light intensity by a factor of $5 \times 10^{-7}$ by the use of optical filters, a power density of $1.26 \times 10^{-11}$ watts/$cm^2$ was obtained. A photometer was used to check filter characteristics in the visible and infrared range and to verify attenuation. Spectral characteristics of the 2800 $^{o}K$ tungsten source were adjusted using a filter with attenuation in the deep red and infrared range. The optical arrangements are shown in Figure 18.

## Electronic Equipment

A calibrated audio oscillator was used to check system response to a 3.3 microvolt 1000 cycle sinusoidal input. The signal, after amplification by the unipolar transistor chopper preamplifier, was displayed on a cathode ray oscilloscope with a 10 millivolts per inch capability. Oscilloscope and oscillator calibration was checked by a Ballantine Voltmeter.

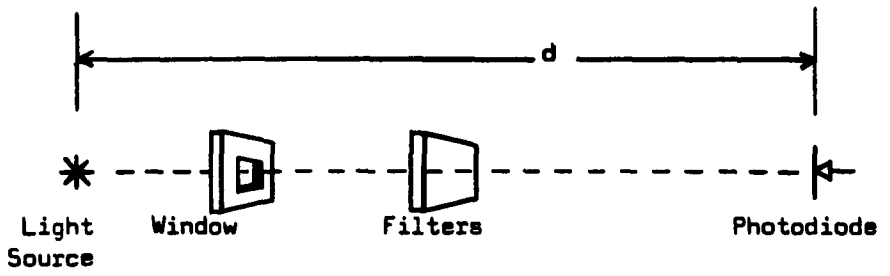


Fig. 18

Placement of Optical Testing Equipment

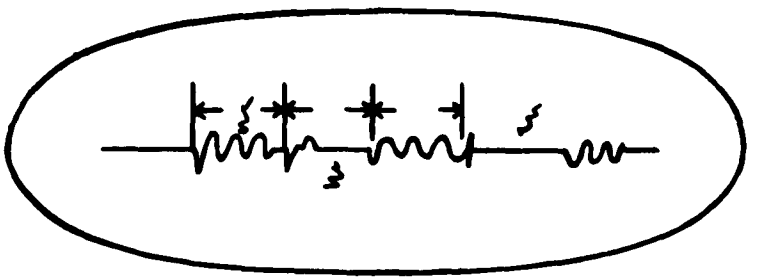

Fig. 19

Oscilloscope Presentation of Output When a 3.3 Microvolt 1000 Cycle Signal is Applied to the First Stage Gate of one Channel

# VIII. Experiments

## Test Conditions

All components and circuitry were tested for proper operation using variable power supplies, resistors, and capacitors in a typical laboratory setup. Testing was initially unsatisfactory at signal levels in the microvolt range due to induced 60 cycle noise. This noise was eliminated by the use of shielded leads, the wiring of non-variable components into shielded chassis, and the removal of noise inducing equipment from the test area. 60 cycle ripple from the transistor power supply was eliminated by filtering.

## Noise Testing

The assembled circuitry was tested for signal-to-noise ratio using a 1000 cycle, 3.3 microvolt sinusoidal signal applied at the gate of the first stage preamplifier of one channel. The signal was clearly distinguishable on the cathode ray oscilloscope and appeared undistorted. High frequency noise, as indicated in Figure 19 was present, but the source could not be determined. As proved by optical testing, if such noise is characteristic of the unipolar transistor low signal amplifier, it will be eliminated by the low pass filters present in the star tracking system.

Optical Testing

Single axis operation of the star tracking system was initially tested by exposing one photodiode to incident light values of $1.26 \times 10^{-11}$ watts/cm$^2$ while the second photodiode was shielded from the light. As the servo amplifier and motor did not require testing, the semi-square wave output of the pre-amplifier under these conditions was taken to the Y channel of a cathode ray oscilloscope. Phase comparisons were made using Lissajous patterns by applying the 400 cycle component from one side of the symetrical multivibrator to the X channel of the CRO. Shifting of the diode exposed to the light shifted the phase of the preamplifier output by approximately $180^{\circ}$, thus proving the theory.

Considerable difficulty was experienced in maintaining equal gain in both channels during laboratory testing. The trimmer resistances used could not be locked in place and appeared to slowly drift. It was therefore necessary to adjust the trimmer resistances several times during performance testing. It is believed that the use of gain stabilized amplifiers, as shown in Figure 12, would eliminate this problem.

To outline the low signal capabilities of the tracking system the value of the incident light level was progressively decreased until the system became unstable. Instability was considered to be reached when system noise became approximately equal to the signal. This was arbitrarily defined as the power

density where one pulse in ten appearing at the summer was of improper phase. System gain was then adjusted so that no servo motor response occurred for signals of magnitude less than this arbitrary cutoff voltage.

Light values, used in optical testing of the system, were derived in the following manner. The intensity of light varies as $k/d^2$ where d is the distance from the light source to the point of measurement. It was therefore possible to determine the light intensity at the photodiode as $I = \frac{I_o F}{d^2}$. The light source used had an intensity $I_o$ of 26.3 lumens = 0.789 watts/cm$^2$ at d = 1 cm. Six optically flat filters which transmitted $1 \times 10^{-6}$ of the incident light were used. A deep red filter with a total transmission of 0.5 was placed in series with the optically flat filters to improve incident light spectral characteristics and provide an F of $5 \times 10^{-7}$, the desired value.

The system became unstable at d = 193 centimeters. Therefore $I_{min} = \frac{(5 \times 10^{-7})(0.789)}{(193)^2} = 1.05 \times 10^{-11}$ watts/cm$^2$.

## IX. Summary of Results

1. The unipolar transistor performed satisfactorily as a low noise, low signal level impedance transformer and amplifier in the circuitry of this report.

2. Electronic chopping, using the special characteristics of the unipolar transistor, is feasible.

3. A space-compatible star tracking system can be built using all solid state components excepting the servo motors.

4. The photovoltaic sensors and preamplifiers of an all solid state star tracking system must be well shielded from stray voltages and be operated with all components in the same temperature environment.

5. Realization of a higher optical gain would simplify the signal-to-noise problems in the system.

## X. Areas for Further Development

1. As only experimental devices of general characteristics were available for testing during the time this thesis was written, the voltage gain of the unipolar stages was not optimized. Information contained in Reference 4 could be utilized to provide design specifications for unipolar transistors more suited to the chopping-impedance transformation function and with a lower driving voltage more compatible with typical satellite power supplies.

2. The unipolar transistor could be applied as an impedance transformer in many low power applications in solid state circuitry, relieving some present requirements for high weight transformers.

3. The optical gain required by present photodiodes could possibly be reduced if higher impedance junctions were used in the devices. The input impedance of the unipolar transistor is so great that an increase in photodiode junction impedances of two orders of magnitude would have little effect on the unipolar transistor amplifier.

4. The optical gain required by the tracking system could perhaps be provided by tapered fiber optics devices. Their use, if feasible, could result in a savings in weight, and reduce problems in the mounting, shock, and vibration areas.

5. As the star tracking system operates on a comparison

basis, it should satisfactorily track a first magnitude star against a second magnitude background. This will be possible if a point differential power density of $1.26 \times 10^{-11}$ watts/$cm^2$ exists for a specified number of seconds of arc about the selected star. If this possibility is proven it will allow the use of desirable, but presently unusable, navigation stars.

6. Testing of the star tracking system proposed in this thesis should be done in a variable temperature, radiative environment to validate its space performance.

## Bibliography


1. ASTIA Document 142761, Correlation of Data Concerning Visible and Near Infrared Radiation from the Night Sky. October 1957, Dayton Ohio.

2. Breed, J. B. Navigation Without Numbers. New York: John Wiley and Sons, 1955.

3. Chin, T. N. "On the Control of Electroluminescent Cells by Unipolar Transistors". Journal of Electronics and Control, 10: 293-306 (April 1961).

4. Chien, C. Y. et all, "Research and Development of Unipolar Transistors". ASD Technical Report 61-506. Dayton Ohio: January 1962.

5. Cholet, P. H. A Solid State Celestial Body Sensor. Interim Technical Report, Philco Corporation 2224-3, Contract No. AF 33(616)-6494, 15 October 1960.

6. Coffey, W. N. "Behavior of Noise Figures in Junction Transistors". Proceedings of the IRE, 46: 495-496 (February 1958).

7. D'Azzo J. and Houpis, C. H. Feedback Control System Analysis and Synthesis, New York: McGraw Hill, 1960.

8. Dever, J. H. "Microcurrent Amplifier". Transactions of the AIEE, Vol 79 part 1 (Communications and Electronics) No. 50: 375-379 (September 1960).

9. Devol, L. and Gable, R. "Limiting Sensitivity of Optical Amplifying Equipment". Fifth Conference of International Commission for Optics, Stockholm Sweden, 1959.

10. Dobrov, E. V. "A Transistor Photoelectric Chopper for DC Operational Amplifiers". Pribbrostroenie, 1959 No. 2 (February). English Translation in Instruments Construction, 1960 February: 9-15.

11. Evans, A. D. "Research on Semiconductor Single Crystal Circuit Development". ASD Technical Report 61-25, WPAFB Ohio: March 1961.

12. Evans, A. D. "Research on Semiconductor Single Crystal Circuit Development". ASD Technical Report 61-120, WPAFB Ohio: September 1961.

13. Hutcheon, I. C. "A Low Drift Transistor Chopper Type DC Amplifier with High Gain and Large Dynamic Range". Proceedings of the Institution of Electrical Engineers, Vol 107B: 451-465 (September 1960).

14. Iles, P. A. "The Present Status of Silicon Solar Cells". IRE Transactions on Military Electronics, Vol Mil-6 No. 1: 5-9 (January 1962).

15. Kapanay, N. S. "Fiber Optics". Scientific American, Vol 203 No. 5: 72-81 (November 1960).

16. NASA Technical Document 608, Satellite Power Sources. Marshall Space Flight Center, July 1961.

17. Oliver, R. M. "Signal to Noise Ratios in Photoelectric Mixing". Proceedings of the IRE, 49: 1960-1 D 61.

18. Philco Corporation, Form L194A, July 1961.

19. Rittner, E. S. "Electron Processes in Photoconductors". Photoconductivity Conference. New York: John Wiley, 1956.

20. Roveti, D. "A Diode Amplifier with a Ten-Gigohm Input Impedance". Electronics. 34: 38-40 (April 22 1961).

21. Runnels, R. W. "Gallium Arsenide Solar Cells". ASD Technical Report 61-88. Dayton: McGregor and Weaver Inc., November 1961.

22. Staff, Philco Research Division, "A Solid State Celestial Body Sensor. Interim Technical Note. AF Contract 33(616)-6494, 13 October 1961.

23. Suran, J. J. and Reibert, F. A. "Two Terminal Analysis of Junction Transistor Multivibrators". Proceedings of the IRE. Vol 144: 26-33 (March 1956).

24. Sylvan, T. P. et all, General Electric Transistor Manual. (Fifth Edition) New York: General Electric Company, 1960.

25. Weis, G. "Synchronous Networks". Transactions of the IRE. Vol AC 7 No. 2: 34-40 (Automatic Control March 1962).

## Appendix A

## Fourier Analysis

The output of the comparitor or summer of Figure 15 is a square wave symetrical to the Y axis and an even function. $B_n$ therefore is zero.

$$e(t) = \frac{a_0}{2} + a_1\cos(nw_0t)\,dt + a_2\cos(nw_0t)\,dt + \ldots\ldots \quad (w_0 = \frac{2pi}{T})$$

$a_n$ = Integral from 0 to T ( $e(t)\cos(nw_0t)\,dt$ ) $n = 0, 1, 2, \ldots$

= Integral from T/4 to 3T/4 ( $2/T\ E_0\cos(nw_0t)\,dt$

$$= \frac{2E_0}{T}\left(\frac{\sin(nw_0t)}{nw_0}\right)\Bigg|_{T/4}^{3T/4}$$

$$= \frac{E_0}{npi}(\sin 3npi/2 - \sin npi/2)$$

$$= \frac{2E_0}{npi} \quad n = 1, 3, 5, 7, \ldots\ldots\ldots$$

$$= 0 \quad n = 2, 4, 6, 8, \ldots\ldots\ldots$$

The magnitude of the 400 cycle component of the output is therefore $\frac{2E_0}{pi}\cos(800pit)$. $(n = 1)$

## Appendix B

## List of Equipment

Audio Oscillator, TS-328 C/U

AC Voltmeter, Model 1051, Ballantine Corporation

Calibrated Light Source, Framm Scientific Company

Cathode Ray Oscilloscope, Model 1735-D, ITT

Dual Channel Cathode Ray Oscilloscope, Model K-26, Electronic Tube Corporation

Galvanometer, Model 599, Weston Corporation

Optical Filters, Bausch and Laumb

Polaroid Scope Camera and Attachments, Polaroid-Land Corp.

Power Supply, Model 103, Kepco Laboratories

Power Supply, Model 712B, Hewlett Packard Company

Recording Spectrophotometer, Carey 14, Applied Physics Corp.

Square Wave Generator, Model 71 Serial 295, Measurement Corp.

Transistor Curve Tracer, Techtronix Corporation

Transistor Power Supply, Model 210, Electronic Research Assoc.

Vacuum Tube Voltmeter, Model 410 B, Hewlett Packard Company

## Vita

James Ray Wolverton was born on 22 February 1934 in Tulsa, Oklahoma, the son of Ray and Georgia Wolverton. After completing his secondary school education in 1951 at Will Rogers High School, Tulsa, Oklahoma, he enlisted in the U. S. Navy. From 1952 to 1956 he attended the United States Naval Academy at Annapolis, Maryland. In June 1956 he was graduated with the degree of Bachelor of Science, and he then received his commission as a Lieutenant in the Regular Air Force. In 1957 he graduated from Pilot Training and in 1958 he completed Fighter Weapons School. His military assignments include duties as a Tactical Fighter Pilot and Air Operations Officer in Misawa, Japan.

Permanent address: 6748 East Fifth Place
Tulsa, Oklahoma

This thesis was typed by James Wolverton.